Supporting Information

MOF-on-MOF Membrane with Cascading Functionality for Capturing Dichromate Ions and P-arsanilic Acid Turn-on Sensing

Ke Zhu, Ruiqing Fan, Jingkun Wu, Bowen Wang, Haoyang Lu, Xubin Zheng, Tiancheng Sun, Shuang Gai, Xuesong Zhou and Yulin Yang**

K. Zhu, Prof. R. Fan, J. Wu, H. Lu, B. Wang, X. Zheng, P. Wang and Prof. Y. Yang
MIIT Key Laboratory of Critical Materials Technology for New Energy Conversion and Storage, School of Chemistry and Chemical Engineering, Harbin Institute of Technology, Harbin 150001, P. R. China
E-mail: fanruiqing@hit.edu.cn and ylyang@hit.edu.cn

Materials and Methods

All the other materials were commercially available reagents of analytical grade. Single-crystal X-ray diffraction (SC-XRD) data of **Cu(I)-tpt** and **Cu(II)-tpt** were obtained by Rigaku SCX-mini diffractometer with graphite monochromatic Mo-Kα radiation (λ = 0.71073 Å). Thermogravimetric analysis (TGA) was carried out on ZRY-2P thermogravimetric analyzer from 40 to 700 °C with a heating rate of 10 °C/min under air atmosphere. Powder X-ray diffraction (PXRD) pattern was obtained using Cu Kα radiation with Shimadzu XRD-6000 X-ray diffractometer. Simulation of PXRD pattern was performed by single crystal data and diffraction crystal module of Mercury program. Scan electron microscope (SEM) image was recorded by Rili SU 8000HSD Series Hitachi New Generation Cold Field Emission. The emission properties were recorded with Edinburgh FLS 920 fluorescence spectrometer equipped with a Peltier-cooled Hamamatsu R928 photomultiplier tube. An Edinburgh Xe900 450 W xenon arc lamp was used as an exciting light source.

Single-Crystal X-Ray Crystal Structure Determination

The X-ray diffraction data taken at room temperature for **Cu(I)-tpt** was collected on a Rigaku R-AXIS RAPID IP diffractometer equipped with graphite-monochromated Mo Kα radiation (λ = 0. 71073 Å). The structure of **Cu(I)-tpt** was solved by direct methods and refined on F^2 by the full-matrix least squares using the SHELXTL-97 crystallographic software. Anisotropic thermal parameters are refined to all of the non-hydrogen atoms. The hydrogen atoms were held in calculated ideal positions on carbon atoms and nitrogen atoms in ligands. The chemical formulas were determined by the combination of single crystal data, TGA results and elemental analysis. The CCDC 1994836 and 2022584 contains the crystallographic data **Cu(I)-tpt** and **Cu(II)-tpt** of

this paper. These data can be obtained free of charge at www.ccdc.cam.ac.uk/ deposit. Crystal structure data and details of the data collection and the structure refinement are listed as Table S1and S3, selected bond lengths and bond angles of **Cu(I)-tpt** and **Cu(II)-tpt** are listed as Table S2 and S4.

■ EXPERIMENTAL SECTION

Adsorption experiments of $Cr_2O_7^{2-}$

All the tests were performed in aqueous solution, and the **Cu(II)-tpt-on-Cu(I)-tpt membrane** (2 cm × 2 cm, The average load of crystals in the membrane is 51.3±0.2 mg) was standby application. Then adsorption kinetic experiment was performed under different initial $Cr_2O_7^{2-}$ concentrations (20, 40 and 60 mg L^{-1}) (the total volume of solution was 200 mL and the pH value was controlled at 7). Adsorption isotherm experiment was investigated at room temperature by immersing **Cu(II)-tpt-on-Cu(I)-tpt membrane** to the solution containing $Cr_2O_7^{2-}$ with different initial concentrations (from 0 to 100 mg L^{-1}) (V = 200 mL and pH = 7). The effects of solution pH value on the adsorption capacity were further studied by simply putting **Cu(II)-tpt-on-Cu(I)-tpt membrane** and $Cr_2O_7^{2-}$ into different pH solutions (from 2 to 11), which were adjusted with HCl or NaOH (the concentration of $Cr_2O_7^{2-}$ was 100 mg L^{-1}, respectively). After the adsorption was completed, all the solutions were taken 2 mL using a pipette. Finally, the concentration of $Cr_2O_7^{2-}$ in the resulting solution was monitored by UV-Vis Absorption Spectrum (UV-Vis).

The adsorption capacity q_t (mg g^{-1}) was calculated by the following equation (1) :

$$q_t = (C_0-C_t)V/M \qquad (1)$$

where C_0, C_t and C_e mean the concentration of $Cr_2O_7^{2-}$ at initial time, at contact time and at equilibrium (mg L^{-1}), respectively. V is the total volume of $Cr_2O_7^{2-}$ solution (L). M represents the amount of **Cu(II)-tpt-on-Cu(I)-tpt** in membrane (g).

The corresponding formulas for pseudo-first-order and pseudo-second-order model were shown as equation (2) and (3):

$$\ln(q_e-q_t) = \ln q_e - k_1 t \quad (2)$$

$$t/q_t = 1/k_2 q_e^2 + t/q_e \quad (3)$$

where q_t and q_e means the adsorption capacity of $Cr_2O_7^{2-}$ at contact time and equilibrium (mg g^{-1}), respectively. k_1 means the rate constant of pseudo-first-order model (min^{-1}), and k_2 represents the equilibrium rate constant of pseudo-second-order equation ($g \cdot mg^{-1} \cdot min^{-1}$).

The corresponding formula for Langmuir and Freundlich model were exhibited as equation (4) and (5):

$$C_e/q_e = 1/q_{max}k_L + C_e/q_{max} \quad (4)$$

$$\ln q_e = \ln k_F + \ln C_e/n \quad (5)$$

where C_e represents the $Cr_2O_7^{2-}$ concentration at equilibrium (mg L^{-1}). q_e is the adsorption capacity of $Cr_2O_7^{2-}$ at equilibrium (mg g^{-1}). q_{max} means the theoretical maximum adsorption capacity (mg g^{-1}). k_L represents the constant of Langmuir model (L mg^{-1}). k_F and n mean the Freundlich constants.

Sensing experiments of p-ASA

The **Cu(II)-tpt-on-Cu(I)-tpt membranes** after adsorption treatment were immersed into different concentrations of p-ASA solutions (5 - 150 $\mu g \cdot L^{-1}$), and then take out it

from the p-ASA solutions. Subsequently, the fluorescence intensity of the **Cu(II)-tpt-on-Cu(I)-tpt membranes** were measured at an excitation wavelength of 340 nm. In order to verify the selectivity of **Cu(II)-tpt-on-Cu(I)-tpt membranes** for p-ASA, various common cations (such as K^+, Na^+, Zn^{2+} etc.), anions (Cl^-, NO_3^-, SO_4^{2-} etc.), organics (glucose, starch, carboxymethylcellulose sodium (NaCMC)), and some other organic-arsonic acid (p-hydroxyphenylarsonic acid (p-HPA), phenyl-arsenic acid (PAA), roxarsone (ROX)) were examined. The concentration of these substances were three times the concentration of p-ASA (the concentration of p-ASA solution was 1mM).

Syntheses of Cu(I)-tpt

The **Cu(I)-tpt** was prepared by solvothermal method. Firstly, CuI (0.019 g, 0.10 mmol) was dissolved in CH_3CN (6 mL) solution, and then $NH_3 \cdot H_2O$ (10 μL) was added. After stirring for 20 minutes, adding the ligand Htpt (0.0213 mg, 0.10 mmol) and continue to stir for another 30 minutes, and finally transfer the mixed suspension to a Teflon-lined stainless steel container (20 mL), place it at 85 °C for 60 hours, and after cooling to room temperature. The colourless block-shaped crystals were obtained (yield: 84%, based on copper metal). Elemental analysis (%): calculated for $CuN_7C_9H_6$ (Mr = 275.76): C, 39.16; H, 2.18; N, 35.54. found: C, 38.87; H, 2.25; N, 35.53.

Syntheses of (Cu(II)-tpt)

The **Cu(II)-tpt** was prepared by solvothermal method. Firstly, $Cu(NO_3)_2 \cdot 3H_2O$ (0.024 g, 0.10 mmol) was dissolved in CH_3OH (6 mL) solution, and then HNO_3 (10 μL) was added. After stirring for 20 minutes, adding the ligand Htpt (0.0213 g, 0.10 mmol) and continue to stir for another 30 minutes, and finally transfer the mixed

suspension to a Teflon-lined stainless steel container (20 mL), place it at 85 °C for 3 days, and after cooling to room temperature. The blue block-shaped crystals were obtained (yield: 84%, based on copper metal). Elemental analysis (%): calculated for $CuN_{14}C_{18}OH_{14}$ (Mr = 569.52): C, 37.92; H, 2.46; N, 34.41. found: C, 37.87; H, 2.45; N, 34.47.

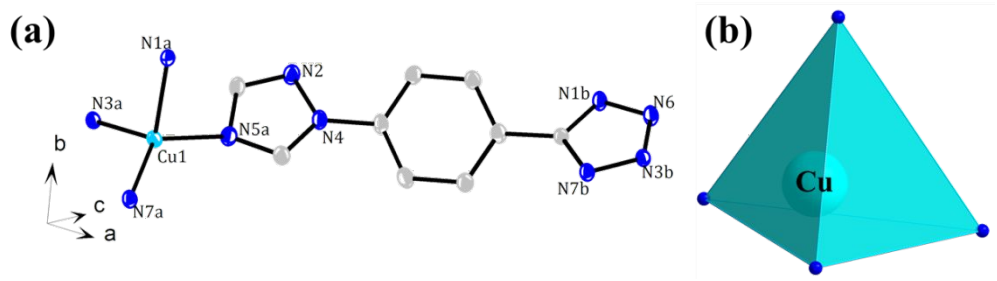

Figure S1. (a) Asymmetric unit of **Cu(I)-tpt** with hydrogen atoms being omitted for clarity. (b) The tetrahedral geometry of Cu^{+}.

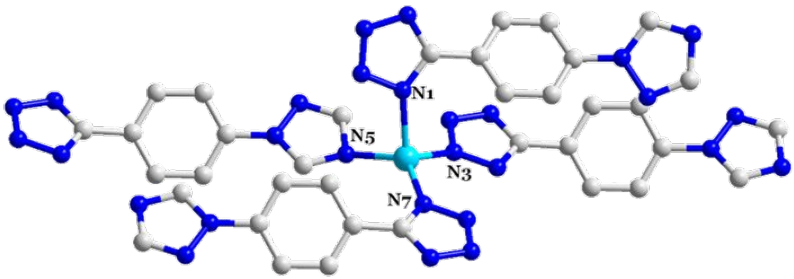

Figure S2. Connection mode of Cu^{+}.

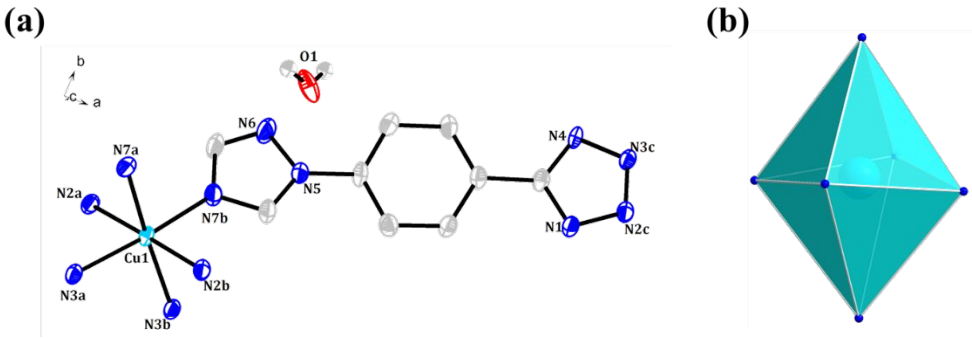

Figure S3. (a) Asymmetric unit of **Cu(II)-tpt** with hydrogen atoms being omitted for clarity. (b) The octahedral geometry of Cu^{2+}.

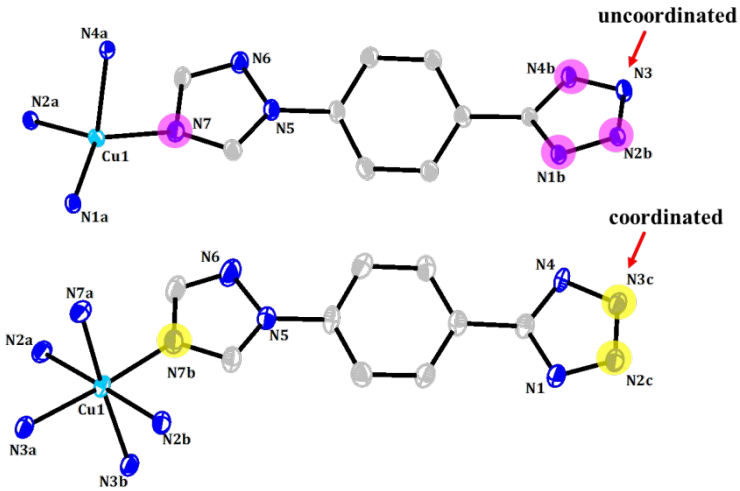

Figure S4. The coordination mode of **Cu(I)-tpt** and **Cu(II)-tpt.**

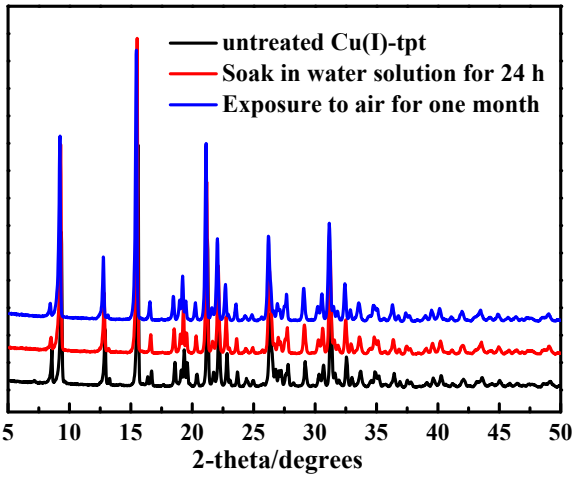

Figure S5. PXRD patterns of **Cu(I)-tpt** under treatment.

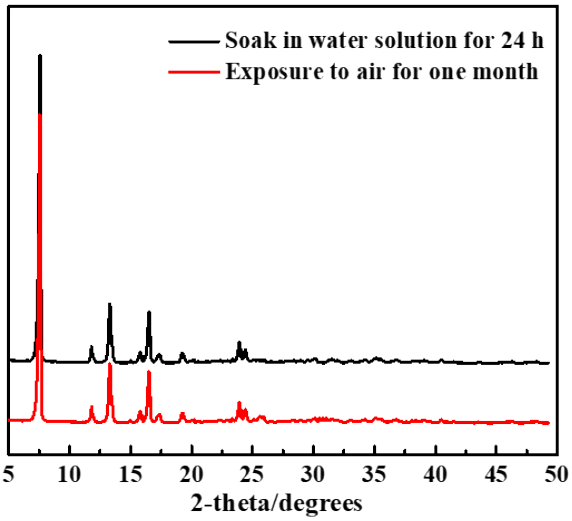

Figure S6. PXRD patterns of **Cu(II)-tpt** under treatment.

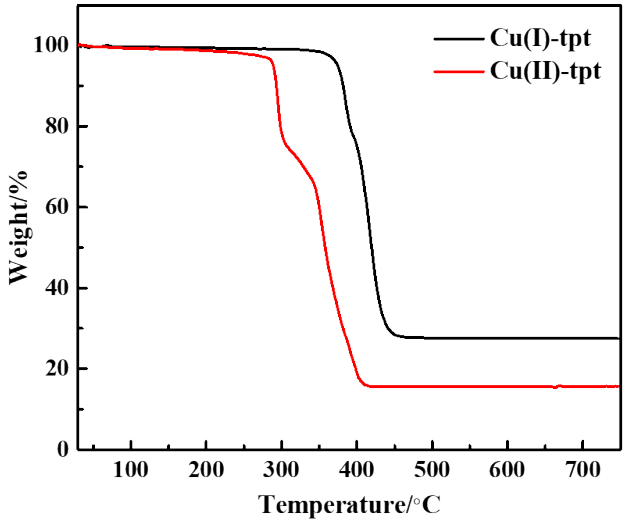

Figure S7. The TG curves of **Cu(I)-tpt** and **Cu(II)-tpt**.

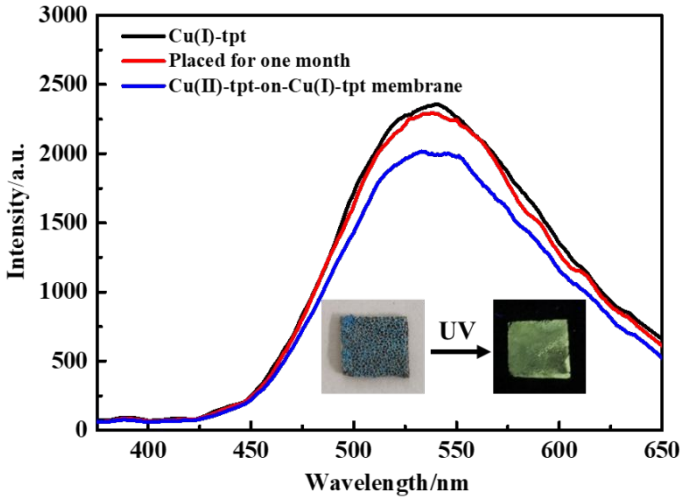

Figure S8. Fluorescence spectra of the **Cu(I)-tpt** and **Cu(II)-tpt-on-Cu(I)-tpt membrane**.

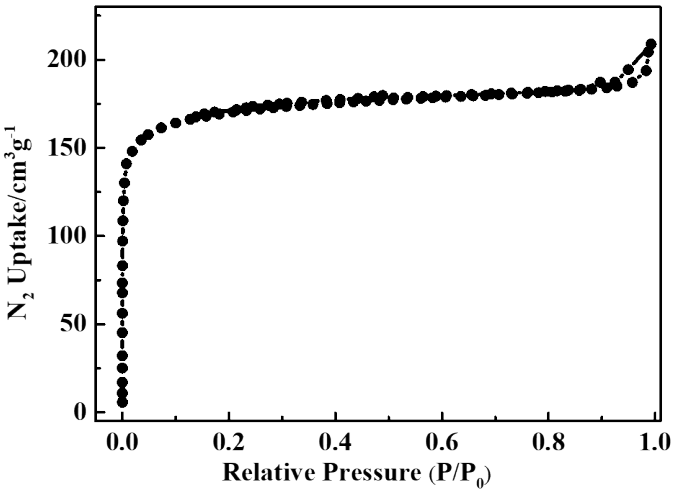

Figure. S9: N2 adsorption and desorption isotherms of **Cu(II)-tpt.**

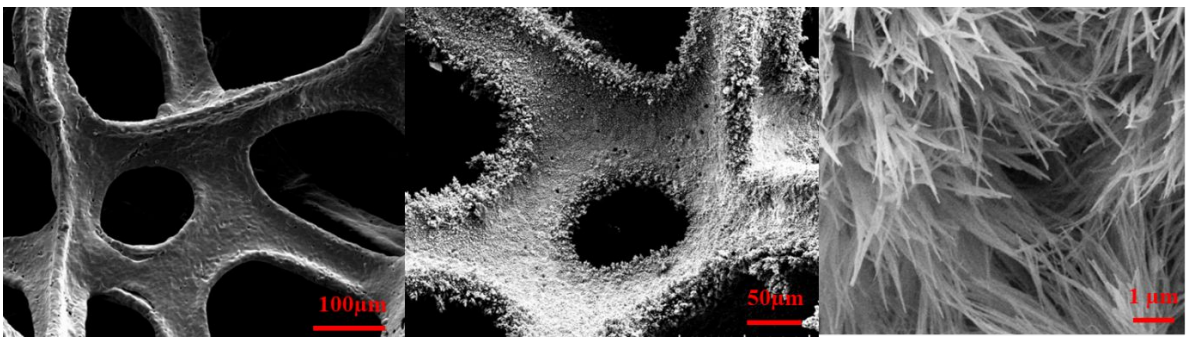

Figure S10. The SEM image of copper foam, electrodeposited copper foam and Cu_2O nanostructure arrays on copper foam.

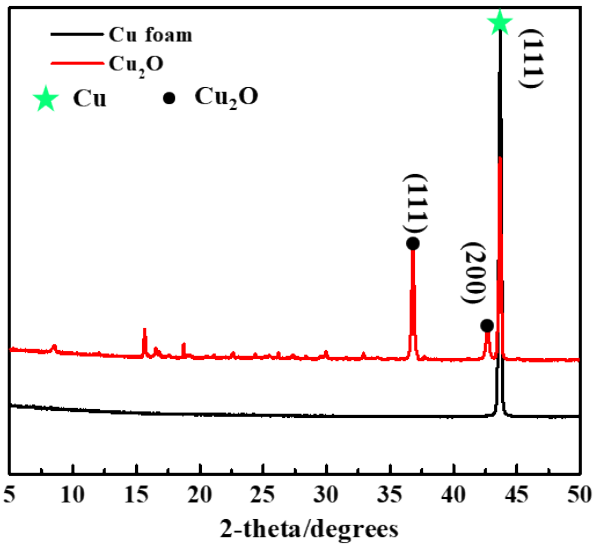

Figure S11. The PXRD pattern of Cu foam and Cu_2O.

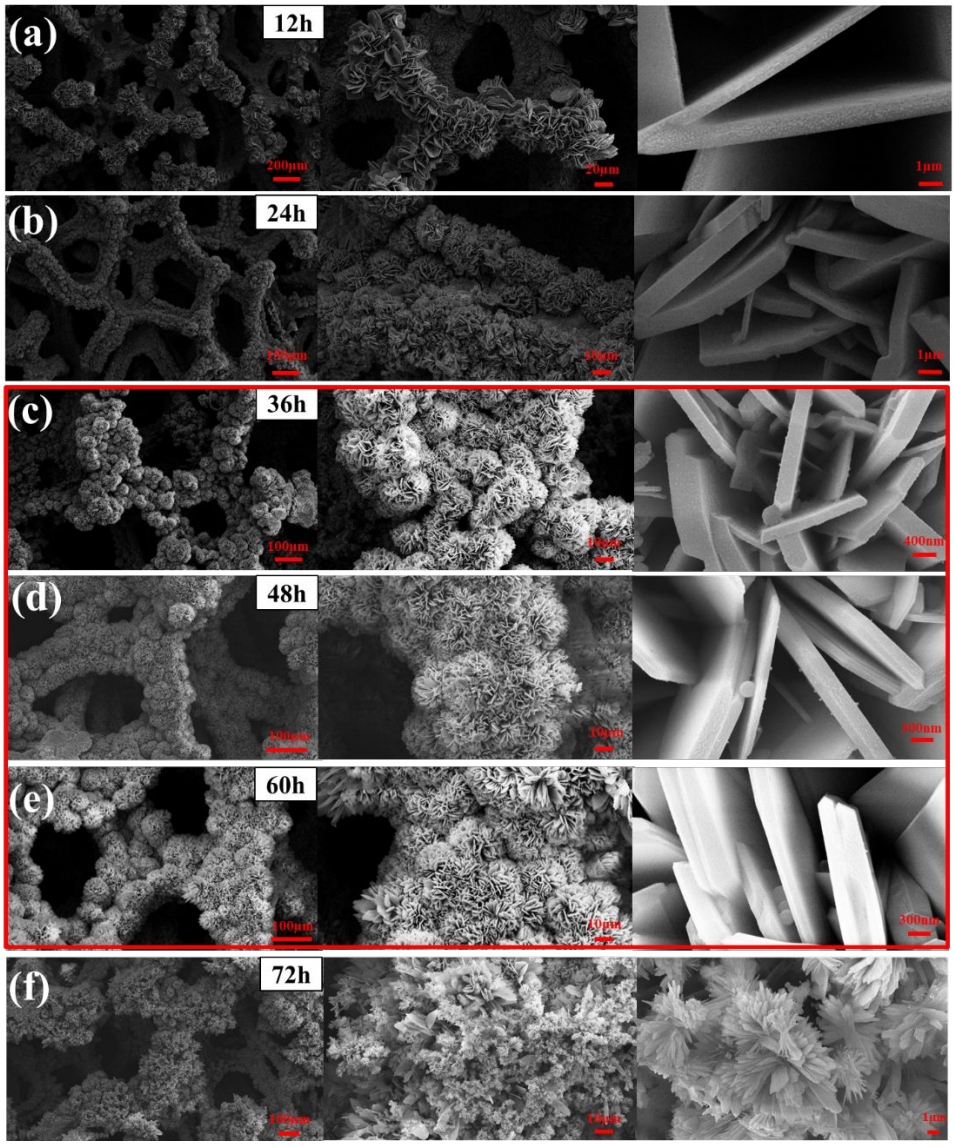

Figure S12. SEM images of synthesized **Cu(I)-tpt** layer for different time periods of in situ solvothermal synthesis: (a) 12 h; (b) 24 h; (c) 36 h; (d) 48 h; (e) 60 h; (f)72h.

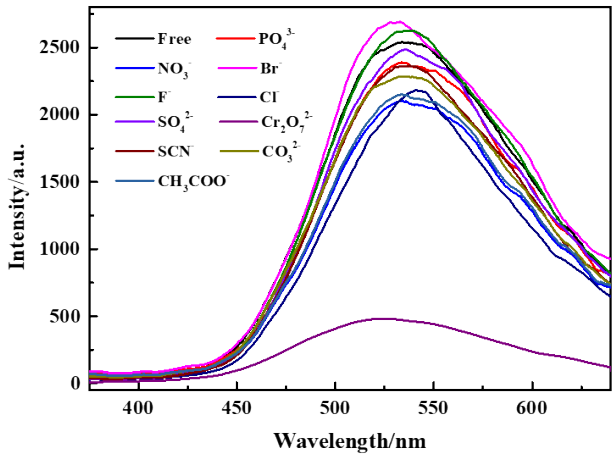

Figure S13. Emission spectra of **Cu(II)-tpt-on-Cu(I)-tpt membrane** under 10 kinds of anions aqueous solutions.

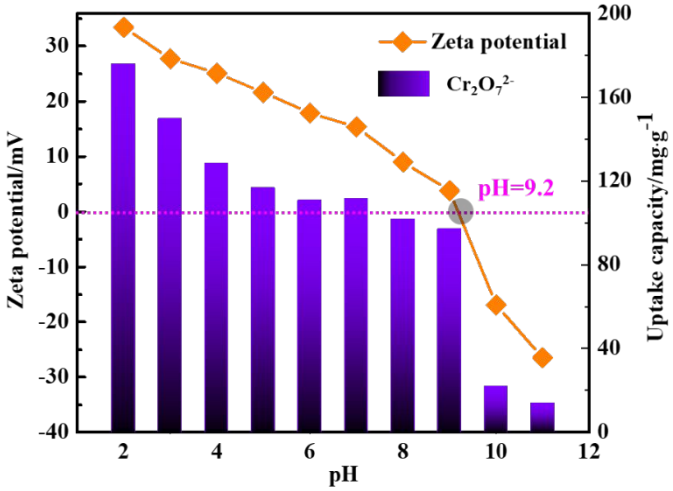

Figure S14. The adsorption performance of $Cr_2O_7^{2-}$ on **Cu(II)-tpt-on-Cu(I)-tpt membrane** at different solution pH and the zeta potential of **Cu(II)-tpt**.

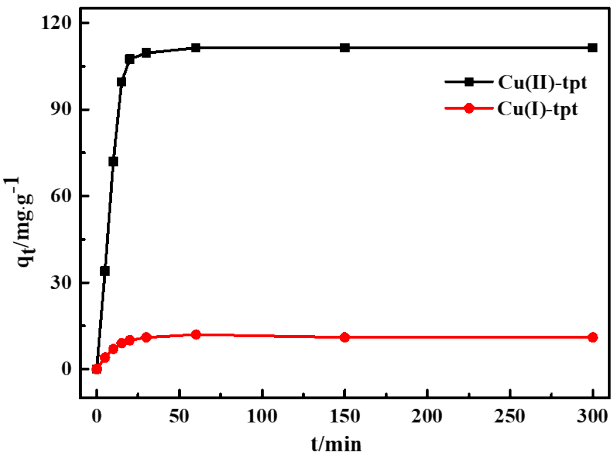

Figure S15. Kinetic curve of **Cu(I)-tpt** and **Cu(II)-tpt** toward $Cr_2O_7^{2-}$ (40 mg L^{-1})

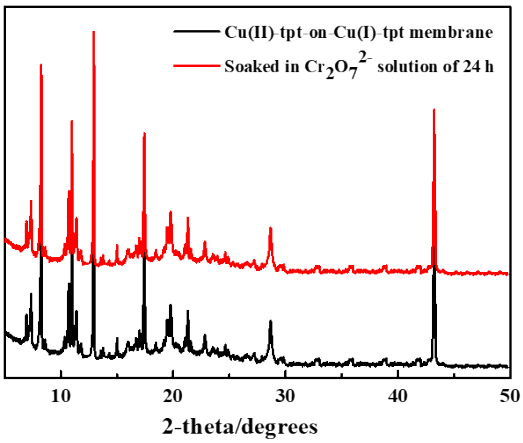

Figure S16. PXRD patterns of **Cu(II)-tpt-on-Cu(I)-tpt membrane** before and after soaked in $Cr_2O_7^{2-}$.

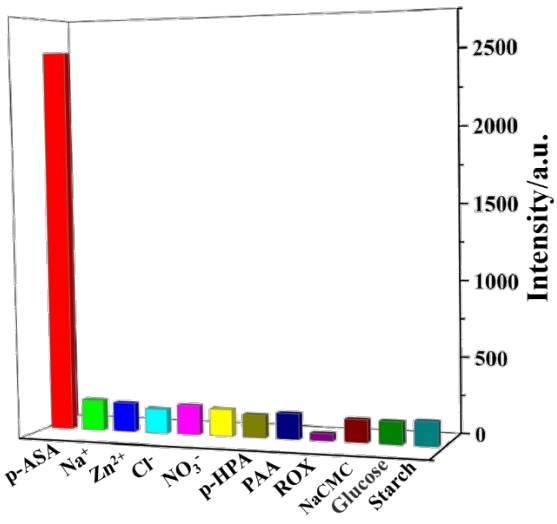

Figure S17. The response of **Cu(II)-tpt-on-Cu(I)-tpt membrane** to different substances.

Table S1. Crystal data and structure refinement parameters of **Cu(I)-tpt**

Identification code	**Cu(I)-tpt**
Empirical formula	$CuN_7C_9H_6$
CCDC	1994836
Formula mass	275.75
Crystal system	Monoclinic
Space group	P2 1/c
a (Å)	9.5702(4)
b (Å)	10.7184(4)
c (Å)	9.0910(3)
α (˚)	90.00
β (˚)	92.5770(10)
γ (˚)	90.00
V (Å3)	931.59(6)
Z	4
Dc/(g cm-3)	1.966
μ (Mo Kα)/mm-1	2.329
F(000)	522
θ range (°)	2.85 – 30.53
Limiting indices	$-13 \leq h \leq 12$
	$-12 \leq k \leq 15$
	$-11 \leq l \leq 12$
Data/Restraints/Parameters	2839 / 0 / 154
GOF on F2	0.919
R1a	0.0380
wR2b	0.1114
R1	0.0548
wR2	0.1296

[a] $R_1 = \sum||F_o| - |F_c|| / \sum|F_o|$; [b] $wR_2 = [\sum[w(F_o^2 - F_c^2)^2] / \sum[w(F_o^2)^2]]^{1/2}$.

Table S2. Selected bond lengths (Å) and bond angles (°) for **Cu(I)-tpt**

Cu(I)-tpt			
Cu(1)-N(7)	1.977(2)	Cu(1)-N(3)	2.0790(19)
Cu(1)-N(5)	2.087(2)	Cu(1)-N(1)	2.100(2)
N(7)-Cu(1)-N(3)	113.37(8)	N(7)-Cu(1)-N(5)	128.27(9)
N(3)-Cu(1)-N(5)	100.23(8)	N(7)-Cu(1)-N(1)	115.37(9)
N(3)-Cu(1)-N(1)	100.96(8)	N(5)-Cu(1)-N(1)	94.08(9)

Table S3. Crystal data and structure refinement parameters of **Cu(II)-tpt**

Identification code	**Cu(II)-tpt**
Empirical formula	$CuN_{64}C_{64}O_8H_{80}$
CCDC	2022584
Formula mass	2128.12
Crystal system	Monoclinic
Space group	C2/c
a (Å)	22.834(2)
b (Å)	14.4584(12)
c (Å)	6.9109(7)
α (˚)	90.00
β (˚)	95.391(4)
γ (˚)	90.00
V (Å3)	2271.5(4)
Z	4
Dc/(g cm-3)	1.556
μ (Mo Kα)/mm-1	1.013
F(000)	1092
θ range (°)	2.82 – 28.27
Limiting indices	–3 0≤ h ≤ 29
	–19 ≤ k ≤ 19
	–9≤ l ≤ 6
Data/Restraints/Parameters	2815 / 0 / 159
GOF on F2	1.221
R1a	0.0695
wR2b	0.1879
R1	0.0999
wR2	0.2070

[a] $R_1 = \sum||F_o| - |F_c|| / \sum|F_o|$; [b] $wR_2 = [\sum[w(F_o^2 - F_c^2)^2] / \sum[w(F_o^2)^2]]^{1/2}$.

Table S4. Selected bond lengths (Å) and bond angles (°) for **Cu(II)-tpt**

Cu(I)-tpt			
Cu(1)-N(7)	2.014(3)	Cu(1)-N(3)	1.999(3)
Cu(1)-N(2)	2.577(4)		
N(3)-Cu(1)-N(3)	89.65(19)	N(3)-Cu(1)-N(7)	90.39(14)
N(3)-Cu(1)-N(7)	90.40(14)	N(7)-Cu(1)-N(7)	90.8(2)
N(3)-Cu(1)-N(7)	171.52(14)	N(3)-Cu(1)-N(2)	93.57(12)
N(3)-Cu(1)-N(2)	85.73(13)	N(7)-Cu(1)-N(2)	85.80(13)
N(7)-Cu(1)-N(2)	94.89(13)	N(3)-Cu(1)-N(2)	85.73(13)
N(3)-Cu(1)-N(2)	93.57(12)	N(2)-Cu(1)-N(2)	179.01(15)

Table S5. The parameters of pseudo-first-order kinetic, pseudo-second-order kinetic, and intraparticle diffusion kinetic of $Cr_2O_7^{2-}$ adsorption.

C (mg/L)	pseudo-first-order		
	q_e(mg/g)	K_1	R^2
20	48.32±0.25	0.13699±0.0032	0.9578
40	131.37±0.96	0.15145±0.0009	0.9552
60	209.98±1.02	0.09923±0.0009	0.9614
C (mg/L)	pseudo-second-order		
	q_e(mg/g)	K_2	R^2
20	59.52±0.31	0.00877±0.0002	0.9997
40	113.38±0.92	0.00229±0.00002	0.9985
60	174.21±1.00	0.00073±0.00002	0.9976

Table S6. Different ratio of two MOFs in **Cu(II)-tpt in Cu(II)-tpt-on-Cu(I)-tpt membrane** and the LOD of p-ASA.

	Cu(I)-tpt M_I/g	**Cu(II)-tpt M_{II}/g**	**M_I : M_I**	**C($Cr_2O_7^{2-}$) /mg L^{-1}**	**LOD(p-ASA) /μg L^{-1}**
Membrane 1	0.0374	0.0054	6.93:1	3.0	0.1068
Membrane 2	0.0379	0.0098	3.87:1	2.5	0.0863
Membrane 3	0.0354	0.0174	2.03:1	2.0	0.0556
Membrane 4	0.0383	0.0368	1.04:1	2.0	0.0572
Membrane 5	0.0376	0.0744	1:1.98	1.5	0.0514
Membrane 6	0.0368	0.1137	1:3.09	/	/